symmetry

IMPACT FACTOR 2.940

CITESCORE 4.9

Article

Hyperbolic Scenario of Accelerating Universe in Modified Gravity

Raja Azhar Ashraaf Khan, Rishi Kumar Tiwari, Jumi Bharali, Amine Bouali, G. Dilara Açan Yildiz and Ertan Güdekli

Special Issue

Application of Symmetry in Gravity Researches

Edited by

Dr. Ghulam Mustafa, Dr. S.K. Maurya and Prof. Dr. Saibal Ray

MDPI

https://doi.org/10.3390/sym15061238

symmetry

MDPI

Article

Hyperbolic Scenario of Accelerating Universe in Modified Gravity

Raja Azhar Ashraaf Khan [1,*], Rishi Kumar Tiwari [2], Jumi Bharali [3], Amine Bouali [4], G. Dilara Açan Yildiz [5] and Ertan Güdekli [6]

[1] Department of Physics, Zhejiang Normal University, Jinhua 321004, China
[2] Department of Mathematics, Government Model Science College, Rewa 486001, India
[3] Department of Mathematics, Handique Girls' College, Guwahati 781001, India
[4] Laboratory of Physics of Matter and Radiation, Mohammed I University, Oujda BP 717, Morocco
[5] Department of Physics, Faculty of Science and Letters, Piri Reis University, Istanbul 34940, Turkey
[6] Department of Physics, Istanbul University, Istanbul 34134, Turkey
* Correspondence: azharashraaf@zjnu.edu.cn

Abstract: Throughout this study, locally rotationally symmetric (LRS) Bianchi type-V space-time is pondered with Tsallis holographic dark energy (THDE) with the Granda–Oliveros (GO) cut-off in the Sáez–Ballester (SB) theory of gravity. A parameterization of the deceleration parameter (q) has been suggested: $q = \alpha - \frac{\beta}{H^2}$. The proposed deceleration parameterization demonstrates the Universe's phase transition from early deceleration to current acceleration. Markov chain Monte Carlo (MCMC) was utilized to have the best-fit value for our model parameter and confirm that the model satisfies the recent observational data. Additional parameters such as deceleration parameter q with cosmographic parameters jerk, snap, and lerk have also been observed physically and graphically. The constructed model is differentiated from other dark energy models using statefinder pair analysis. Some important features of the model are discussed physically and geometrically.

Keywords: Bianchi type-V space-time; Tsallis holographic dark energy; deceleration parameterization

Citation: Khan, R.A.A.; Tiwari, R.K.; Bharali, J.; Bouali, A.; Yildiz, G.D.A.; Güdekli, E. Hyperbolic Scenario of Accelerating Universe in Modified Gravity. *Symmetry* **2023**, *15*, 1238. https://doi.org/10.3390/sym15061238

Academic Editor: Ghulam Mustafa, S.K. Maurya, Saibal Ray, Vasilis K. Oikonomou

Received: 10 February 2023
Revised: 15 May 2023
Accepted: 30 May 2023
Published: 9 June 2023

1. Introduction

Available statistics of astronomical data [1–3] reveal that the Universe is expanding at a faster rate. Its acceleration is driven by an unidentified substance called dark energy (DE). DE has low pressure and a high energy density (ρ). The Universe is generally supposed to comprise 4.9% normal matter, 26.8% dark matter (DM), and 68.3% DE. The cosmological constant Λ is the most straightforward candidate for DE, as it accommodates the equation of state (EOS) $p = \omega\rho$ with negative EOS parameter $\omega = -1$. Nonetheless, the DE contender has fine-tuning and cosmic coincidence challenges. To address these issues, various DE alternatives have been presented, such as holographic DE [4–12], tachyon [13,14], k-essence [15], quintom [16], quintessence [17], phantom [18–22], and others. Numerous different gravitational theories have been presented in order to comprehend the Universe's current accelerated phase. Starobinsky [23] and Kerner [24] proposed another way by changing the geometrical element of Einstein's equation of motion, named modified gravity theory; $f(R)$; where R is denoted by scalar curvature [25,26]; $f(T)$ theory, here T denoted by torsion scalar [27–29]; $f(G)$ theory, where G is represented by Gauss–Bonnet [30,31]; $f(R,T)$ theory [32], wherein R is the Ricci scalar and T is the trace of the energy–momentum tensor. Scalar–tensor theories of gravity [33,34] and extra-dimensional theories [35] are various modified theories of gravity. The holographic principle (HP) is incorporated into cosmology [36,37] to analyze the dark energy composition of the Universe. The authors of [38] established this idea in the domain of black hole (BH) science, whereas [39] expanded that to string theory. According to the HP, a system's entropy varies not only with its dimension but additionally with its porous structure [37]. This might

alternatively be interpreted as the degree of freedom (DOF) of a spatial region residing not throughout the bulk but just at the region's edge, with the number of DOF per Planck region being less than unity. A connection among ultraviolet (UV) as well as infrared (IR) curves has been postulated using this approach, implying that perhaps the scale of the system really should not transcend the scale associated with the mass of a BH U̇sing this correlation, Li [37] proposed the HDE density concept $\rho_{de} = 3c^2 M_{pl}^2 L^{-2}$ where c, M_{pl}, and L represent the HDE constant, the reduced Planck constant, and the IR cut-off, respectively. There was consideration of the lowered Planck constant and the IR cut-off with $M_{pl}^{-2} = 8\pi G$. Several IR cut-offs have been designed based on the consistency of HDE with current data, such as the Hubble particles, event horizons, topological age of the Universe, Ricci scalar, Granda–Oliveros (GO), and higher derivatives of the Hubble parameter H [37,40–43], among others. The HP proposes a correlation in the context of the DE issue: ρ_{de} is proportionate to the Hubble scale squared, i.e., $\rho_{de} \propto H^2$. Recently, [42,44] suggested a kind of holographic density $\rho_{de} \approx \tau H^2 + \eta \dot{H}$ where τ and η are parameters that must adhere to the constraints imposed by present observational data. To understand the present accelerated stage of the Universe, a new HDE called Tsallis HDE (THDE) has been proposed using Tsallis generalized entropy $S_\delta = \gamma A^\delta$ [45–51], wherein A is the BH area, γ is an unidentified constant, and δ signifies the Tsallis or non-extensive parameter. For $\gamma = \frac{1}{G}$ and $\delta = 1$, the Bekenstein entropy has been restored. The authors of [52] created a connection between the system entropy S, IR cut-off L, and UV cut-off Λ as $L^3\Lambda^3 \leq S^{3/4}$. Substituting the entropy from $S_\delta = \gamma A^\delta$ and taking the area as $A = 4\pi L^2$, we obtain $\Lambda^4 \leq \gamma(4\pi)^\delta L^{2\delta-4}$, where Λ^4 represents the vacuum ρ. In accordance with the HDE concept, Λ^4 is assumed as DE's ρ. Using this inequality, the ρ of the THDE model is obtained as $\rho_{de} = DL^{2\delta-4}$, where D is an unknown parameter [46]. There are multiple options for the IR cut-off L particularly, such as Hubble length H^{-1} [53], particle horizon [54], future event horizon [55], and Granda–Oliveros (GO) cut-off [42,44], etc. The dimension scale is composed of H and $\dot{H}$ in general, i.e., $L_{GO} = \left(\tau H^2 + \eta \dot{H}\right)^{-1/2}$, with τ and η being two dimensionless constants, integrating THDE density and GO magnitude as $\rho_{de} = D\left(\tau H^2 + \eta \dot{H}\right)^{-\delta+2}$ [42]. The finest values for τ and η are $\tau \sim 0.8502$ and $\eta \sim 0.4817$ for the flat case [56]. Sáez–Ballester theory (SBT) is one of the numerous adaptations to General Relativity. It has been demonstrated to be adaptable enough to handle the dark energy problem while also accommodating reconstructing circumstances [57–59]. SBT also discussed the Bianchi Cosmology in [58,59] replicating the Universe's shift from a decelerating to an accelerating phase. Yet, in [59] it was viewed as a basis to explore Tsallis HDE. Currently, SBT is now assumed to be in agreement with precision cosmology evidence.

This current work investigates the SBT of gravity [34], which is a scalar-tensor idea. Throughout this theory, the metric is paired with a dimensionless scalar field. Considering that the scalar field is dimensionless, an anti-gravity domain occurs in this theory [34,60,61]. This theory's foundation might offer a solution to the vanishing matter conundrum in non-flat FRW cosmologies. Various studies [62–66] explored the nature of the cosmos under the SBT of gravity in numerous cosmological models. The investigation of Bianchi type-V cosmological models seems important in the understanding of the Universe because these models include isotropic special circumstances that allow for unrestricted degrees anywhere at the point in astronomical terms. Bianchi V universes are indeed a natural generalization of the open FRW model that finally become isotropic. Furthermore, at later stages, this cosmological model tends towards isotropy and therefore enables the formation of galaxies. We have studied the different forms of deceleration parameters of several researchers [67–69]. In this paper, we introduce a new form of the deceleration parameter (there is some recent work considering the parameterization of the deceleration parameter [70–73]) in SB theory in the framework of Bianchi type-V space–time with a new deceleration parameter $q = \alpha - \frac{\beta}{H^2}$ in SB gravity, where α, β, and H are negative constants, positive constants, and the Hubble parameter, respectively. This paper is organized as follows: Section 2 is devoted to metrics that describe the geometry of the Universe and its field equations. Section 3 contains the solutions to the field equations. In Section 4, the

best-fit value of the free parameter is found using $H(z)$, pantheon, and baryon acoustic oscillations (BAO). The cosmographic parameter is discussed in Section 5. The statefinder diagnostic is covered in Section 6, and Sections 7 and 8 cover energy conditions and the Om diagnostic, respectively. Section 9 concludes the study with results and remarks.

2. Basic Equations Governing the Model

The anisotropic and spatially homogeneous Bianchi type-V space–time is given by

$$ds^2 = dt^2 - A^2dx^2 - B^2e^{2x}\left(dy^2 + dz^2\right) \tag{1}$$

wherein cosmic scale factors A and B are solely function of cosmic time t. In (1986), Sáez and Ballester [34] proposed a scalar–tensor theory of gravity, known as the Sáez–Ballester theory. In this theory, the metric is coupled with a dimensionless scalar field in a different way. This coupling provides a reasonable description of the weak field in which an accelerated expansion regime reflects further.

The Sáez–Ballester Lagrangian is a type of scalar–tensor theory that was proposed as a modification of the Brans–Dicke theory. It is given by:

$$L = \frac{1}{16\pi G}\left[\phi R - \omega(\phi)(\partial\phi)^2\right] - V(\phi) \tag{2}$$

where ϕ is a scalar field, R is the scalar curvature, G is the gravitational constant, $\omega(\phi)$ is a function of the scalar field that determines the strength of the scalar field coupling to matter, and $V(\phi)$ is the scalar field potential.

To write the Sáez–Ballester Lagrangian in terms of standard scalar–tensor theory, we need to make some modifications. Specifically, we need to express $\omega(\phi)$ in terms of a new scalar field, Φ, and then rewrite the Lagrangian in terms of Φ. This can be done by introducing a conformal transformation of the metric:

$$g'_{\mu\nu} = \Omega^2 g_{\mu\nu} \tag{3}$$

where $\Omega = e^{\sqrt{2/3}\Phi}$ and $g_{\mu\nu}$ is the original metric. This transformation maps the Sáez–Ballester Lagrangian to a new Lagrangian in terms of Φ:

$$L' = \frac{1}{16\pi G}\left[R - \frac{2g'^{\mu\nu}\partial_\mu\Phi\partial_\nu\Phi}{3\Omega^2}\right] - V(\phi) \tag{4}$$

Note that the new Lagrangian has a canonical kinetic term for the scalar field Φ, and the coupling between the scalar field and matter is determined by the function $\omega(\phi)$, which can be expressed in terms of Φ as:

$$\omega(\Phi) = \frac{3}{2}\left[\frac{d\ln\Omega}{d\Phi}\right]^2 - \frac{3}{2} \tag{5}$$

Substituting this expression into the Lagrangian, we obtain the Sáez–Ballester Lagrangian in terms of standard scalar–tensor theory:

$$L = \frac{1}{16\pi G}\left[R - \frac{2g'^{\mu\nu}\partial_\mu\Phi\partial_\nu\Phi}{3\Omega^2}\right] - V(\phi) - \frac{1}{16\pi G}\omega(\Phi)g'^{\mu\nu}\partial_\mu\psi\partial_\nu\psi \tag{6}$$

where ϕ is the scalar field, R is the scalar curvature, G is the gravitational constant, Φ is the new canonical scalar field, $\omega(\Phi)$ is a function of the scalar field that determines the strength of the scalar field coupling to matter, ψ is the matter field, and $\Omega = e^{\sqrt{2/3}\Phi}$ is the conformal factor. The revised Einstein field equations in Sáez–Ballester of standard scalar–tensor theory can be obtained by varying the action $S = \int d^4x\sqrt{-g}L$ with respect to the metric $g_{\mu\nu}$. This yields:

$$G_{\mu\nu} = \frac{8\pi G}{c^4} T_{\mu\nu} + \frac{1}{\phi}\partial_\mu\phi\partial_\nu\phi - \frac{1}{2}g_{\mu\nu}\left[\frac{1}{\phi}\partial^\rho\phi\partial_\rho\phi + V(\phi)\right] + \frac{1}{\Omega^2}\left[\partial_\mu\Phi\partial_\nu\Phi - \frac{1}{2}g_{\mu\nu}\partial^\rho\Phi\partial_\rho\Phi\right] \tag{7}$$

where $G_{\mu\nu}$ is the Einstein tensor, $T_{\mu\nu}$ is the stress-energy tensor of matter, c is the speed of light, ϕ is the scalar field, Φ is the new canonical scalar field, $V(\phi)$ is the scalar field potential, and $\Omega = e^{\sqrt{2/3}\Phi}$ is the conformal factor. Note that the presence of the scalar field ϕ and the new scalar field Φ in the Einstein field equations leads to modifications of the standard Einstein equations, reflecting the additional degrees of freedom present in scalar–tensor theories.

$$\bar{T}_{\mu\nu} = \rho_m u_\mu u_\nu \tag{8}$$

$$\dot{T}_{uv} = (p_{de} + \rho_{de})u_\mu u_\nu - p_{de}g_{\mu\nu} \tag{9}$$

where ρ_m and ρ_{de} are the energy density of DM and THDE, correspondingly.

$$T_{\mu\nu} = \bar{T}_{\mu\nu} + \dot{T}_{\mu\nu} \tag{10}$$

The equation is fulfilled by the scalar field φ,

$$2\varphi^n\varphi^{;\mu}_{;\mu} + n\varphi^{n-1}\varphi_{,k}\varphi^{,k} = 0 \tag{11}$$

in which the semicolon and comma represent covariant and partial derivative with regard to cosmic time t. The revised EFE and scalar field equation in moving coordinates results in the subsequent set of equations of motion as

$$2\frac{\ddot{B}}{B} + \frac{\dot{B}^2}{B^2} - \frac{1}{A^2} - \frac{\omega}{2}\varphi^n\dot{\varphi}^2 = -\omega_{de}\rho_{de} \tag{12}$$

$$\frac{\ddot{A}}{A} + \frac{\ddot{B}}{B} + \frac{\dot{A}\dot{B}}{AB} - \frac{1}{A^2} - \frac{\omega}{2}\varphi^n\dot{\varphi}^2 = -\omega_{de}\rho_{de} \tag{13}$$

$$2\frac{\dot{A}\dot{B}}{AB} + \frac{\dot{B}^2}{B^2} - \frac{3}{A^2} + \frac{\omega}{2}\varphi^n\dot{\varphi}^2 = \rho_m + \rho_{de} \tag{14}$$

$$\frac{\dot{A}}{A} - \frac{\dot{B}}{B} = 0 \tag{15}$$

$$\ddot{\varphi} + \dot{\varphi}\left(\frac{\dot{A}}{A} + 2\frac{\dot{B}}{B}\right) + \frac{n}{2}\frac{\dot{\varphi}^2}{\varphi} = 0 \tag{16}$$

in which the above dot (.) signifies the derivative with respect to cosmic time t. One gets it by integrating Equation (15) and supposing the integrating constant is unity.

$$A = B \tag{17}$$

One can get the following set of independent field equations by substituting Equation (17) into Equations (12)–(14) and (16).

$$2\frac{\ddot{A}}{A} + \frac{\dot{A}^2}{A^2} - \frac{1}{A^2} - \frac{\omega}{2}\varphi^n\dot{\varphi}^2 = -\omega_{de}\rho_{de} \tag{18}$$

$$3\frac{\dot{A}^2}{A^2} - \frac{3}{A^2} + \frac{\omega}{2}\varphi^n\dot{\varphi}^2 = \rho_m + \rho_{de} \tag{19}$$

$$\ddot{\varphi} + \dot{\varphi}\left(3\frac{\dot{A}}{A}\right) + \frac{n}{2}\frac{\dot{\varphi}^2}{\varphi} = 0 \tag{20}$$

3. Solutions of Field Equations

The parameter V denotes the spatial volume.

$$V = a^3 = A^3 \tag{21}$$

Here, a is denoted by the average scale factor. The THDE density in terms of the GO cut-off is described as in [42]. There are multiple options for the IR cut-off L such as Hubble length, particle horizon, future event horizon, GO cut-off, etc. In this work, THDE density in terms of GO cut-off is

$$\rho_{de} = D\left(\tau H^2 + \eta \dot{H}\right)^{-\delta+2} \tag{22}$$

Furthermore, a new deceleration parameter q has been proposed:

$$q = \alpha - \frac{\beta}{H^2} \tag{23}$$

where in H denotes the Hubble parameter and α and β denote negative and positive constants.The authors of [74–77] discuss the underlying reasoning for adopting such an assumption. Scale factor $a(t)$ could be derived by integrating Equation (23) and utilizing the definition of deceleration parameter $q = \frac{-\ddot{a}}{aH^2}$.

$$a = A = \left[\sinh\left\{(\sqrt{(1+\alpha)\beta})t + t_0\right\}\right]^{\frac{1}{1+\alpha}} \tag{24}$$

with t_0 being an integrating constant; H and q are the Hubble and deceleration parameters, correspondingly.

$$H = \sqrt{\frac{\beta}{1+\alpha}}\coth\left\{(\sqrt{(1+\alpha)\beta})t + t_0\right\} \tag{25}$$

$$H(z) = \sqrt{\frac{\beta}{1+\alpha}}\left[(1+z)^{2(1+\alpha)} + 1\right]^{1/2} \tag{26}$$

$$H(z) = H_0\left[\frac{1}{2}\left\{(1+z)^{2(1+\alpha)} + 1\right\}\right]^{1/2} \tag{27}$$

and

$$q = \alpha - (1+\alpha)\tanh^2\left\{(\sqrt{(1+\alpha)\beta})t + t_0\right\} \tag{28}$$

The THDE density ρ_{de} is obtained as

$$\rho_{de} = D\left[\left(\frac{\tau\beta}{1+\alpha}\right)\coth^2\left\{(\sqrt{(1+\alpha)\beta})t + t_0\right\} - \eta\beta\,\mathrm{csch}^2\left\{(\sqrt{(1+\alpha)\beta})t + t_0\right\}\right]^{2-\delta} \tag{29}$$

Integrating Equation (20) and using the value of A from Equation (24), the scalar field φ acquired as

$$\varphi^{\frac{n+2}{2}} = c_1\left(\frac{n+2}{2}\right)\int \frac{dt}{\left[\sinh\left\{(\sqrt{(1+\alpha)\beta})t+t_0\right\}\right]^{\frac{3}{1+\alpha}}} + c_2 \tag{30}$$

wherein c_1 and c_2 represent integrating constants. The EOS parameter ω_{de} and the matter-energy density ρ_m could be derived via Equations (18) and (19) as

$$\rho_m = \left(\frac{3\beta}{1+\alpha}\right)\coth^2\left\{(\sqrt{(1+\alpha)\beta})t+t_0\right\} - \frac{3}{\left[\sinh\left\{(\sqrt{(1+\alpha)\beta})t+t_0\right\}\right]^{\frac{2}{1+\alpha}}} + \frac{\omega c_1^2}{2\left[\sinh\left\{(\sqrt{(1+\alpha)\beta})t+t_0\right\}\right]^{\frac{6}{1+\alpha}}} - \rho_{de} \tag{31}$$

$$p_{de} = \omega_{de}\rho_{de} = 2\beta\,\mathrm{csch}^2\left\{(\sqrt{(1+\alpha)\beta})t+t_0\right\} - \left(\frac{3\beta}{1+\alpha}\right)\coth^2\left\{(\sqrt{(1+\alpha)\beta})t+t_0\right\} + \frac{1}{\left[\sinh\left\{(\sqrt{(1+\alpha)\beta})t+t_0\right\}\right]^{\frac{2}{1+\alpha}}} + \frac{\omega c_1^2}{2\left[\sinh\left\{(\sqrt{(1+\alpha)\beta})t+t_0\right\}\right]^{\frac{6}{1+\alpha}}} \tag{32}$$

$$\omega_{de} = \frac{1}{\rho_{de}}[2\beta\,\mathrm{csch}^2\left\{(\sqrt{(1+\alpha)\beta})t+t_0\right\} - \left(\frac{3\beta}{1+\alpha}\right)\coth^2\left\{(\sqrt{(1+\alpha)\beta})t+t_0\right\} + \frac{1}{\left[\sinh\left\{(\sqrt{(1+\alpha)\beta})t+t_0\right\}\right]^{\frac{2}{1+\alpha}}} + \frac{\omega c_1^2}{2\left[\sinh\left\{(\sqrt{(1+\alpha)\beta})t+t_0\right\}\right]^{\frac{6}{1+\alpha}}}] \tag{33}$$

4. Data Analysis

4.1. Data Description

In this section, the model parameters are constrained using three different forms of observational datasets. We used the H(z) datasets of 57 observations, the Pantheon dataset of 1048 measurements, and 17 uncorrelated BAO measurements to get the best value for the suggested model parameters. Open-source tools Polychord [78] and GetDist [79] are used to build the Markov chain Monte Carlo (MCMC) [80]. The total χ^2 function of the $H(z)$ + Pantheon + BAO combination is defined as

$$\chi^2_{tot} = \chi^2_{H(z)} + \chi^2_{SN} + \chi^2_{BAO}. \tag{34}$$

4.1.1. $H(z)$ Dataset

A large number of observational datasets must be employed to achieve considerable restrictions on the model parameters. In this research, $H(z)$ observations are used to limit the model parameters. In general, Hubble data may be calculated by calculating the BAO in the radial direction of galaxy clusters [81] or by the differential age technique, which additionally yields the redshift dependence of the Hubble parameter as

$$H(z) = -\frac{1}{1+z}\frac{dz}{dt}, \tag{35}$$

wherein dz/dt is calculated proportionally using two moving galaxies. The study uses 57 Hubble readings, which cover a redshift range of $0.07 \leqslant z \leqslant 2.42$, to estimate the model's

parameters. The chi-square function is used to compare the theoretical predictions of the model with observations.

$$\chi^2_H = \sum_{i=1}^{57} \frac{[H_{th}(z_{i,}) - H_{obs}(z_i)]^2}{\sigma^2_{H(z_i)}}, \tag{36}$$

where H_{th} , H_{obs}, and $\sigma_{H(z_i)}$ denotes the model prediction, observed value of Hubble rate, and standard error at the redshift z_i, respectively. The Hubble function numerical values for the appropriate redshifts are shown in [73].

4.1.2. Pantheon Dataset

The measurement of type Ia supernovae (SNIa) allows us to determine cosmic expansion. SNIa have shown to be one of the most effective approaches for understanding the nature of dark energy so far. Many supernova datasets have been generated in recent years [82–86]. The Pantheon sample had been recently updated [87]. The former dataset comprises 1048 spectroscopically validated SNIa spanning the $0 < z < 2.3$ redshift range. SNIa are also astronomical objects that serve as reference candles for calculating relative distances. As a result, SNIa samples are mixed with the distance modulus $\mu = m - M$, where m represents the apparent magnitude of a single SNIa. The SNIa measures' chi-square is given by

$$\chi^2_{SN} = \Delta\mu^T \cdot \mathbf{C}^{-1}_{SN} \cdot \Delta\mu \tag{37}$$

where $\mathbf{C}_{SN}$ is represented by a covariance matrix, and $\Delta\mu = \mu_{obs} - \mu_{th}$, where μ_{obs} signifies the measured distance modulus of a certain SNIa. The theoretical distance modulus is represented as μ_{th} and calculated as

$$\mu_{th}(z) = 5\log_{10}\frac{D_L(z)}{(H_0/c)Mpc} + 25, \tag{38}$$

Thus, H_0 corresponds to the present Hubble rate, and c indicates the speed of light. The luminosity distance, D_L, is defined for the flat Friedmann–Lemaitre–Robertson–Walker (FLRW) Universe as described in the following:

$$D_L(z) = (1+z)H_0 \int_0^z \frac{dz'}{H(z')}. \tag{39}$$

Although free parameters are limited at the same time, i.e., by utilizing the Pantheon sample,

$$\chi^2_{SN} \quad = \quad \Delta\mu^T \times \mathbf{C}^{-1}_{Pantheon} \times \Delta\mu.$$

4.1.3. Baryon Acoustic Oscillations

We picked 17 BAO [88] measures from the largest BAO dataset of 333 measurements because considering the whole catalog of BAO might result in considerable inaccuracy because of data correlations; therefore, we chose a representative subset to minimize errors. Transverse BAO experiments produce measurements of $D_H(z)/r_d = c/H(z)r_d$ with a comoving angular diameter distance [89,90].

$$D_M = \frac{c}{H_0} S_k\left(\int_0^z \frac{dz'}{E(z')}\right), \tag{40}$$

where

$$S_k(x) = \begin{cases} \frac{1}{\sqrt{\Omega_k}}\sinh\left(\sqrt{\Omega_k}x\right) & \text{if} \quad \Omega_k > 0 \\ x & \text{if} \quad \Omega_k = 0 \\ \frac{1}{\sqrt{-\Omega_k}}\sin\left(\sqrt{-\Omega_k}x\right) & \text{if} \quad \Omega_k < 0. \end{cases} \tag{41}$$

We also consider the angular diameter distance $D_A = D_M/(1+z)$ and $D_V(z)/r_d$. These correspond to the combination of the BAO peaked coordinates and the sound horizon r_d at the drag epoch. Furthermore, we could immediately derive "line-of-sight" (or "radial") observations from the Hubble parameter.

$$D_V(z) \equiv \left[zD_H(z)D_M^2(z)\right]^{1/3}. \tag{42}$$

5. Cosmography

The parameters indicating deceleration q, jerk j, snap s, and lerk l will be addressed in succession. They can be derived by taking the Hubble parameter's derivative.

5.1. Deceleration Parameter

The deceleration parameter (DP) q quantifies the rate at which the inflation factor slows down. A positive q number reflects the usual decelerating model, whereas a negative q value predicts inflation.

$$q = \frac{(\alpha+1)(z+1)^{2\alpha+2}}{(z+1)^{2\alpha+2}+1} - 1 \tag{43}$$

5.2. Jerk Parameter

The jerk parameter j is defined as

$$j = \frac{\dddot{a}}{aH^3}. \tag{44}$$

For our model, the jerk parameter j takes the form

$$j = \frac{\alpha(2\alpha+1)(z+1)^{2\alpha+2}+1}{(z+1)^{2\alpha+2}+1} \tag{45}$$

5.3. Snap Parameter

The snap parameter s is defined as

$$s = \frac{a^4}{aH^4}. \tag{46}$$

For our model, the snap parameter s takes the form

$$s = -\frac{(2\alpha-1)(\alpha+1)^2}{2(z+1)^{2\alpha+2}+(z+1)^{4\alpha+4}+1} + \frac{2\alpha(4\alpha+1)(\alpha+1)}{(z+1)^{2\alpha+2}+1} - \alpha(2\alpha+1)(3\alpha+2) \tag{47}$$

5.4. Lerk Parameter

The lerk parameter l is defined as

$$l = \frac{a^5}{aH^5}. \tag{48}$$

For our model, the lerk parameter l takes the form

$$\begin{aligned} l = {} & \frac{(2\alpha(8\alpha+1)+1)(\alpha+1)^2}{2(z+1)^{2\alpha+2}+(z+1)^{4\alpha+4}+1} - \frac{10\alpha(2\alpha+1)^2(\alpha+1)}{(z+1)^{2\alpha+2}+1} \\ & + \alpha(2\alpha+1)(3\alpha+2)(4\alpha+3) \end{aligned} \tag{49}$$

Snap and lerk parameters give helpful directions for the emergence of sudden future singularities [91].

6. Statefinder Parameters

Although distinct DE models share the identical current value of the deceleration and Hubble parameters, those parameters cannot distinguish across DE models [92]. For this purpose, we introduce two dimensionless parameters r and s, as well as merging the Hubble and deceleration parameters, which are represented as

$$r = \frac{\dddot{a}}{aH^3} \tag{50}$$

$$s = \frac{r-1}{3\left(q-\frac{1}{2}\right)} \tag{51}$$

The fixed point $(r,s) = (1,0)$ represents ΛCDM; $(r,s) = (1,1)$ represents the standard cold dark matter (SCDM) model; and $s > 0$ and $r < 1$ represent the region of phantom and quintessence DE eras.

In this model, $\{r,s\}$ parameters take the form

$$r = \frac{\alpha(2\alpha+1)(z+1)^{2\alpha+2}+1}{(z+1)^{2\alpha+2}+1} \tag{52}$$

$$s = \frac{2\left(2\alpha^2+a-1\right)(z+1)^{2\alpha+2}}{3(2\alpha-1)(z+1)^{2\alpha+2}-9} \tag{53}$$

The first statefinder parameter r is also known as jerk parameter j. Almost all current cosmological observations [92] can be summarized as $j = 1$.

7. Energy Conditions

The energy conditions are fundamental concepts used to understand the behavior of geodesics in the Universe, and they can be derived from the Raychaudhuri equations. In the literature, there are different energy conditions that are expressed as linear combinations of energy density and pressure. These include the weak energy condition (WEC), dominant energy condition (DEC), and strong energy condition (SEC) [93–96]. Researchers have extensively studied energy conditions in various theories of gravity, and their implications have been investigated by different authors [97,98]. The WEC, DEC, and SEC represent different criteria based on the relationship between energy density and pressure in a given physical system.

$$\rho_{de} \geq 0 \tag{54}$$

$$\rho_{de} + p_{de} \geq 0 \tag{55}$$

$$\rho_{de} + 3p_{de} \geq 0 \tag{56}$$

The WEC was utilized to restrict the Universe's expansion history [99–105]. The WEC additionally tells us that the energy density is not only non-increasing but also positive. The dominant energy condition (DEC) is useful in proving the positive mass theorem [106]. The Hawking Penrose singularity conjecture is based on SEC [107]. Again, $\omega_{de} = \frac{p_{de}}{\rho_{de}} < -1$ for phantom DE models. This implies that $\rho_{de} + p_{de} < 0$. The authors of [18,108] pointed out that Condition 2 is violated. They [18,108] also investigated phantom DE models and explored that phantom DE models violate both Conditions 2 and 3. The energy conditions for our model are represented in Figure 1. WEC (orange line) is satisfied whereas DEC (red line) and SEC (purple line) are violated.

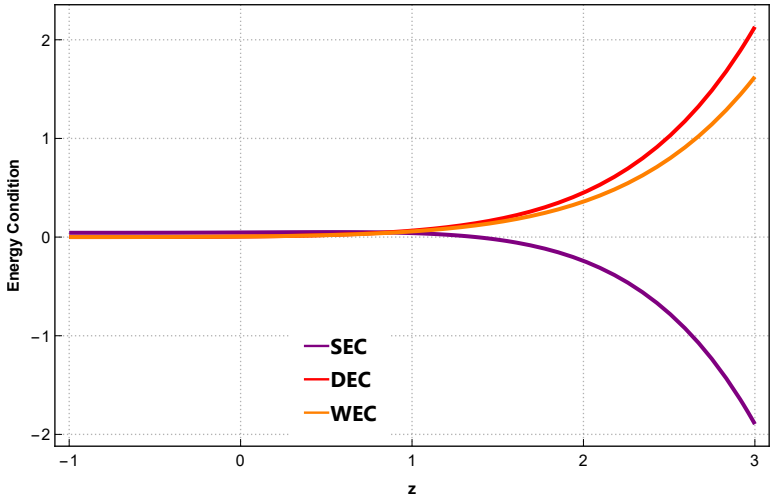

Figure 1. Evolution of energy condition parameter in terms of redshift.

8. Om Diagnostic

This refers to a geometrical formalism in which the Hubble parameter yields a null test for the ΛCDM model [109]. The Om diagnostic also efficiently differentiates several DE models from ΛCDM by the slope variation of $Om(z)$. A quintessence or phantom model can be acquired through either a positive or negative slope of the diagnostic parameter, respectively. Furthermore, a constant slope with respect to redshift depicts a DE model corresponding to the cosmological constant. For a flat universe, one can define $Om(z)$ as

$$Om(z) = \frac{\left(\frac{H(z)}{H_0}\right)^2 - 1}{(1+z)^3 - 1}. \tag{57}$$

For this model, $Om(z)$ is obtained as

$$Om(z) = \frac{(z+1)^{2\alpha+2} - 1}{2((z+1)^3 - 1)} \tag{58}$$

The slope variation of Om(z) versus redshift is shown in Figure 2. For the obtained model, for the whole redshift range, the model stays in the quintessence region as the value of Om stays positive.

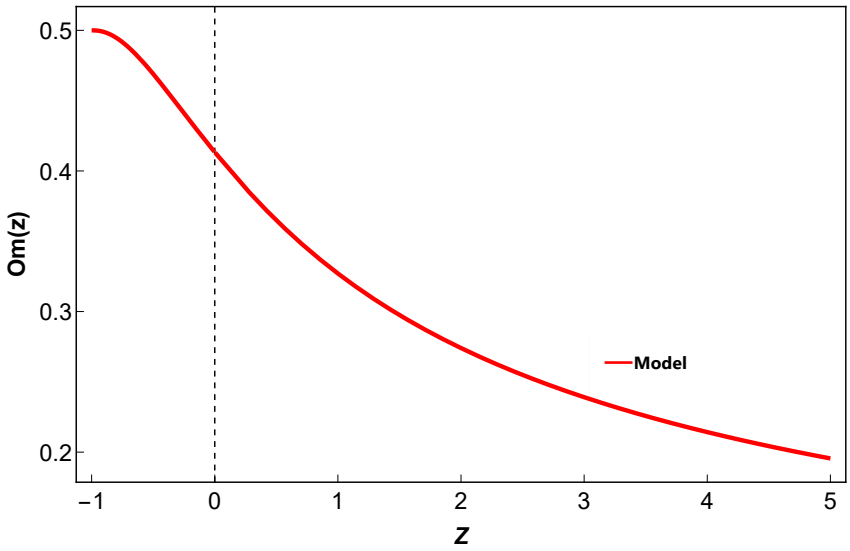

Figure 2. Evolution of Om diagnostic profile.

9. Conclusions and Results

Figure 3 shows the 1σ and 2σ confidence contours obtained from using the $H(z)$ + SC + BAO dataset, and Figures 4 and 5 show curve fitting of the model with 57 Hubble measurements and 1048 type 1a supernova with 1σ and 2σ errors bands and the standard ΛCDM paradigm. Figure 6 indicates the redshift-dependent deceleration parameter using the best-fit value of the model parameter, suggesting that the Universe is evolving out of an early matter-dominated stage toward the de Sitter phase $q = -1$ as $t \to \infty$. The best fit-values of MCMC model are given in Table 1. The cosmographic parameter can be observed in Figures 7–9. Figures 10 and 11 show trajectories of the $s - r$ plane initiate at the ΛCDM fixed point $(r = 1, s = 0)$ and, eventually, both profiles show the model stays in quintessence. In Figure 1, WEC is fulfilled, whereas DEC and SEC are breached, according to an examination of energy conditions. The infringement of DEC and SEC shows that our Universe is saturated with phantom fluid and that exotic stuff exists, as studied by [110]. From Figure 12, we see that the EoS parameter starts with a positive value in the past, remains negative as $z \to 0$, and finally attains the value -0.962 as $z \to -1$, again suggesting the presence of dark energy. Figure 2 shows the Om diagnostic profile of the obtained model, indicating it stays in the quintessence region.

The spatially homogenous and anisotropic Bianchi type-V space–time in the Sáez–Ballester theory of gravity is being studied in this paper. A new deceleration parameter parameterization with GO cut-off was proposed. Cosmological quantities were explored in conjunction with the cosmographic parameter. Energy conditions, stability, and statefinder analysis were also covered. The MCMC approach was used to constrain the model parameters using $H(z)$ datasets, Pantheon datasets, and BAO datasets. The obtained cosmological model may become a mathematically viable alternative. It might also provide new insights and a deeper understanding of the complex link among mathematical notions, frameworks, and physical reality.

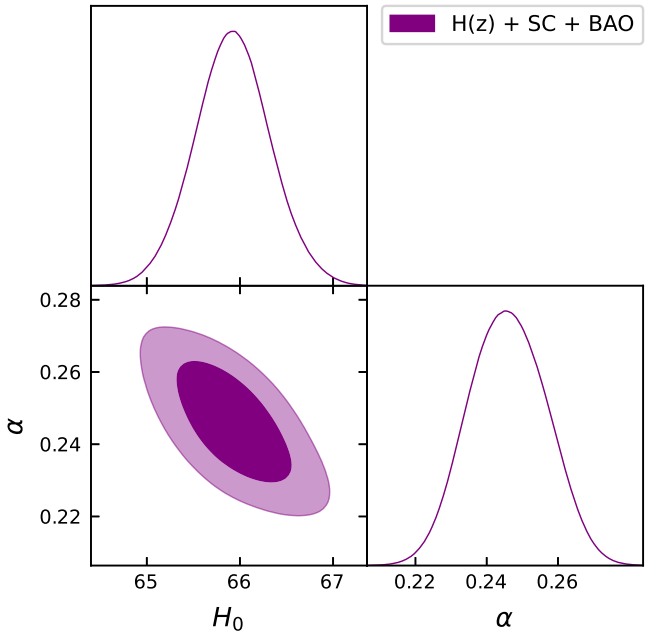

Figure 3. This figure corresponds to 1σ and 2σ confidence contours obtained from $H(z)$ + SC + BAO dataset obtained for the emergent model.

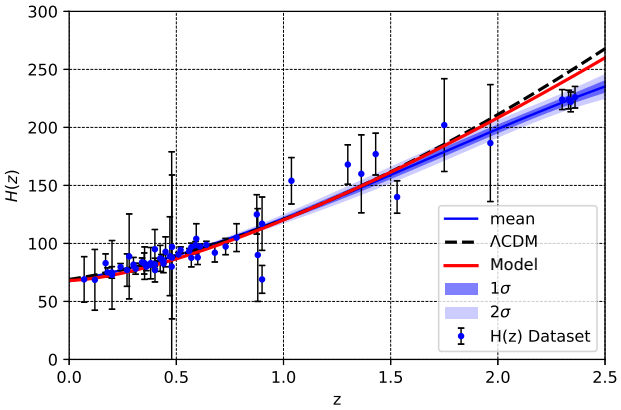

Figure 4. Theoretical curve of Hubble function $H(z)$ of the model shown with a red line and ΛCDM model shown with a black dotted line with $\Omega_{m0} = 0.3$ and $\Omega_\Lambda = 0.7$, against $H(z)$ measurements shown in blue dots with their corresponding error bars with 1σ and 2σ error bands.

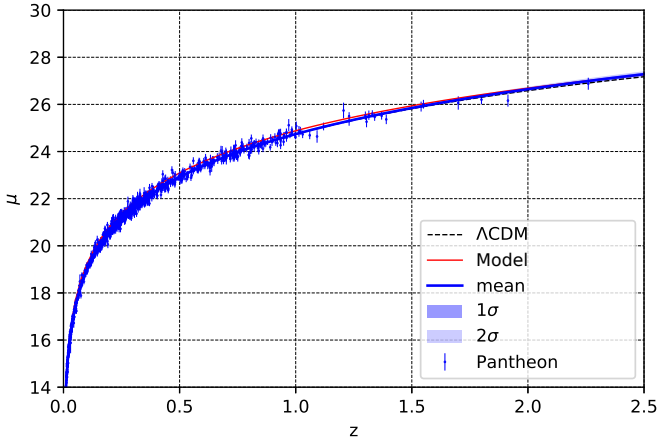

Figure 5. Theoretical curve of distance modulus $\mu(z)$ of the model shown with a red line and ΛCDM model shown with a black dotted line with $\Omega_{m0} = 0.3$ and $\Omega_\Lambda = 0.7$, against type Ia supernova data shown with blue dots with their corresponding errors bars with 1σ and 2σ error bands.

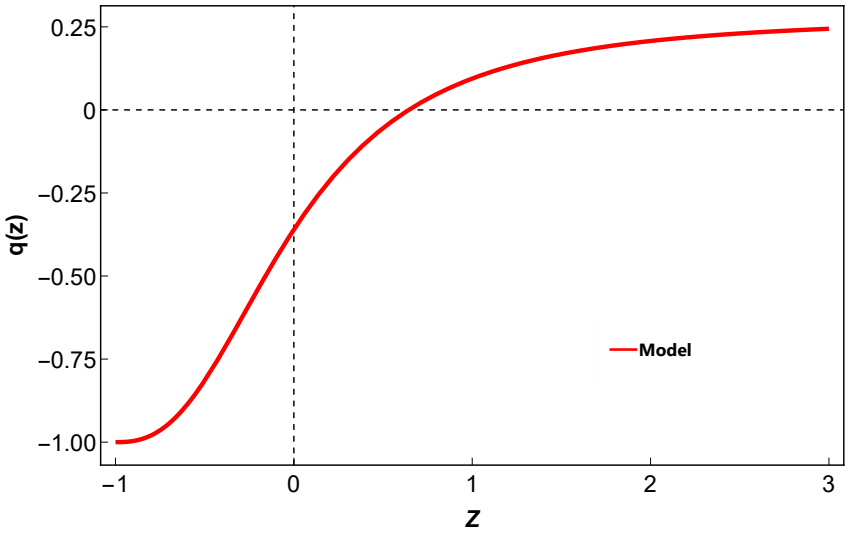

Figure 6. Evolution of deceleration parameter with respect to redshift.

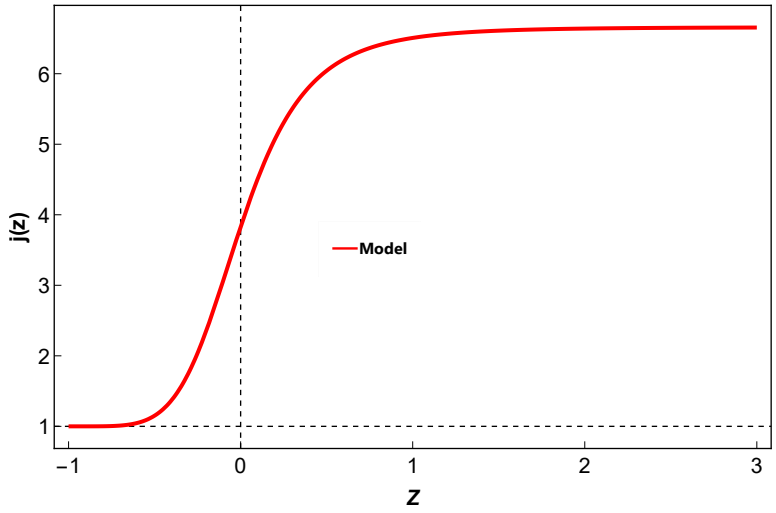

Figure 7. Evolution of jerk parameter with respect to redshift.

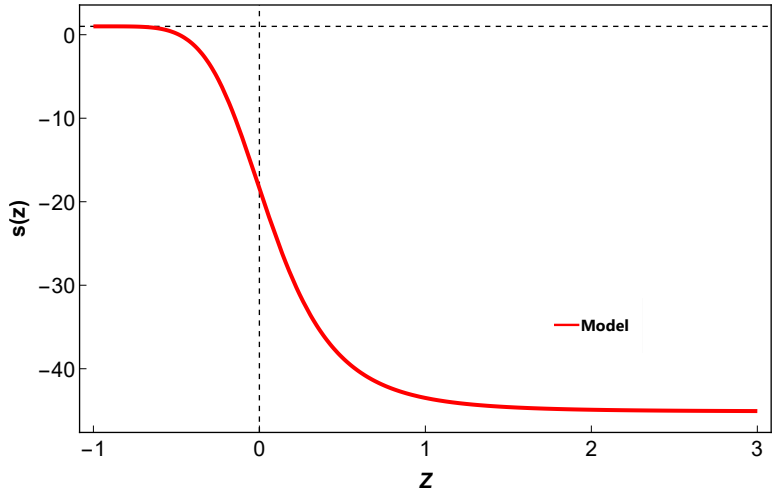

Figure 8. Evolution of snap parameter with respect to redshift.

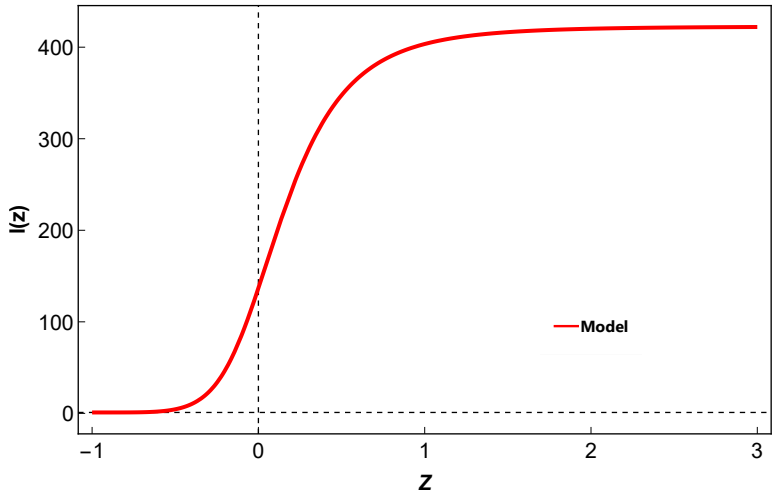

Figure 9. Evolution of lerk parameter with respect to redshift.

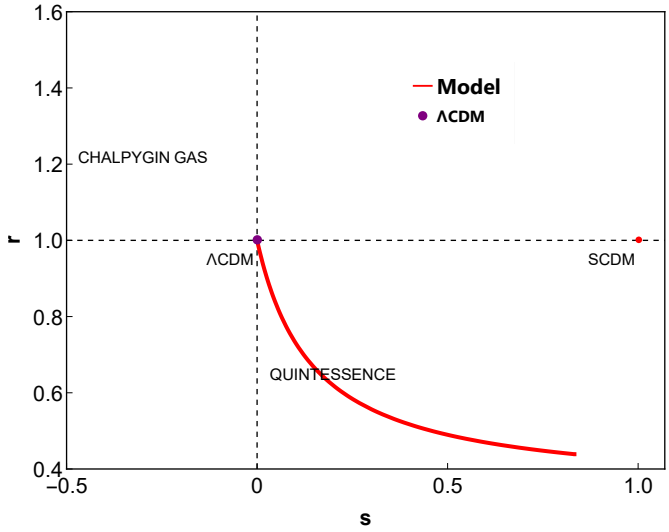

Figure 10. Evolution of $\{s, r\}$ profile.

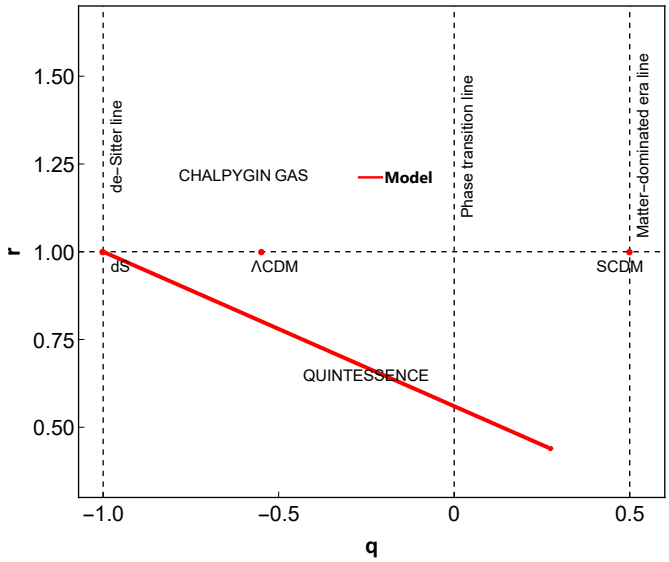

Figure 11. Evolution of $\{q, r\}$ profile.

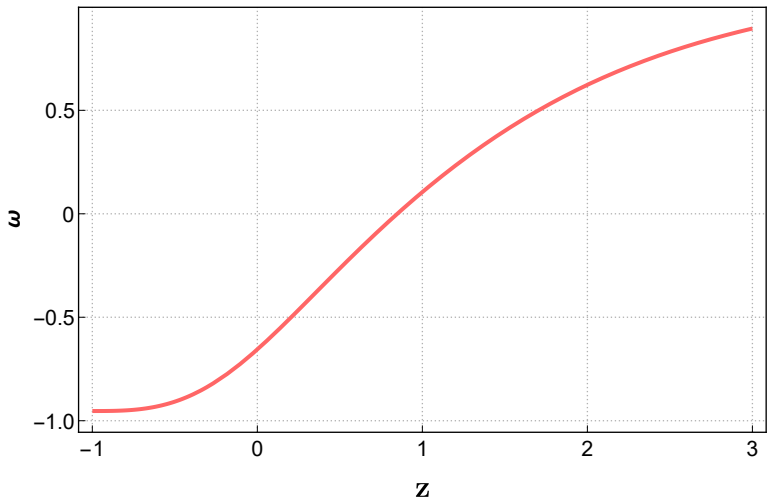

Figure 12. Evolution of equation of state in terms of redshift.

Table 1. MCMC Results.

Model	Parameters	Best-Fit Value
Model 1	H_0	$65.922882^{+0.368984}_{-0.368984}$
	α	$0.245918^{+0.011007}_{-0.011007}$

Author Contributions: Methodology, R.A.A.K., J.B., A.B., G.D.A.Y. and E.G.; Software, R.A.A.K. and G.D.A.Y.; Validation, E. G.; Investigation, R.K.T.; Resources, J.B. and E.G.; Data curation, R.A.A.K., J.B. and A.B.; Writing—original draft, R.A.A.K.; Supervision, R.K.T. and E.G.; Project administration, R.K.T. and A.B.; Funding acquisition, G.D.A.Y. All authors have read and agreed to the published version of the manuscript.

Funding: R.A.A. Khan Acknowledge the Postdoctoral fellowship and startup grant (No. ZC304022916) funded by the Zhejiang Normal University.

Institutional Review Board Statement: Not applicable.

Informed Consent Statement: Not applicable.

Data Availability Statement: There are no observational data related to this article. The necessary calculations and graphic discussion can be made available on request.

Acknowledgments: R.A.A. Khan is very thankful to Gao Xianlong from the Department of Physics, Zhejiang Normal University, for his kind support and help during this research.

Conflicts of Interest: The authors declare no conflict of interest.

References

1. Riess, A.G.; Filippenko, A.V.; Challis, P.; Clocchiatti, A.; Diercks, A.; Garnavich, P.M.; Gilliland, R.L.; Hogan, C.J.; Jha, S.; Tonry, J.; et al. Observational evidence from supernovae for an accelerating universe and a cosmological constant. *Astron. J.* **1998**, *116*, 1009–1038. [CrossRef]
2. Perlmutter, S.; Aldering, G.; Goldhaber, G.; Knop, R.A.; Nugent, P.; Castro, P.G.; Deustua, S.; Fabbro, S.; Goobar, A.; Groom, D.E.; et al. Measurements of Ω and Λ from 42 high redshift supernovae. *Astrophys. J.* **1999**, *517*, 565–586. [CrossRef]
3. Sherwin, B.D.; Dunkley, J.; Das, S.; Appel, J.W.; Bond, J.R.; Carvalho, C.S.; Devlin, M.J.; Dünner, R.; Essinger-Hileman, T.; Fowler, J.W.; et al. Evidence for dark energy from the cosmic microwave background alone using the Atacama Cosmology Telescope lensing measurements. *Phys. Rev. Lett.* **2011**, *107*, 021302. [CrossRef] [PubMed]
4. Bouhmadi-Lopez, M.; Errahmani, A.; Ouali, T. The cosmology of an holographic induced gravity model with curvature effects. *Phys. Rev. D* **2011**, *84*, 083508.
5. Bargach, A.; Bargach, F.; Ouali, T. Dynamical system approach of non-minimal coupling in holographic cosmology. *Nucl. Phys. B* **2019**, *940*, 10–33.
6. Weinberg, S. The cosmological constant problem. *Rev. Mod. Phys.* **1989**, *61*, 1. [CrossRef]
7. Copeland, E.J.; Sami, M.; Tsujikawa, S. Dynamics of dark energy. *Int. J. Mod.* **1989**, *11*, 1.
8. Nojiri, S.; Odintsov, S.D. Unifying phantom inflation with late-time acceleration: Scalar phantom–non-phantom transition model and generalized holographic dark energy. *Gen. Relativ. Gravit.* **2006**, *38*, 1285–1304. [CrossRef]
9. Nojiri, S.; Odintsov, S.D.; Paul, T. Barrow entropic dark energy: A member of generalized holographic dark energy family. *Phys. Lett. B* **2022**, *825*, 136844. [CrossRef]
10. Nojiri, S.; Odintsov, S.D.; Oikonomou, V.; Paul, T. Unifying holographic inflation with holographic dark energy: A covariant approach. *Phys. Rev. D* **2020**, *102*, 023540. [CrossRef]
11. Nojiri, S.; Odintsov, S.D.; Paul, T. Different faces of generalized holographic dark energy. *Symmetry* **2021**, *13*, 928. [CrossRef]
12. Nojiri, S.; Odintsov, S.D.; Paul, T. Early and late universe holographic cosmology from a new generalized entropy. *Phys. Lett. B* **2022**, *831*, 137189. [CrossRef]
13. Sen, A. Tachyon matter. *J. High Energy Phys.* **2002**, *2002*, 65. [CrossRef]
14. Bouabdallaoui, Z.; Errahmani, A.; Bouhmadi-Lopez, M.; Ouali, T. Constraints on tachyon inflationary models with an AdS/CFT correspondence. *Phys. Rev. D* **2016**, *94*, 123508.
15. Chiba, T. Tracking k-essence. *Phys. Rev. D* **2002**, *66*, 063514. [CrossRef]
16. Guo, Z.K.; Piao, Y.S.; Zhang, X.; Zhang, Y.Z. Cosmological evolution of a quintom model of dark energy. *Phys. Lett. B* **2005**, *608*, 177–182. [CrossRef]
17. Sami, M.; Padmanabhan, T. Viable cosmology with a scalar field coupled to the trace of the stress tensor. *Phys. Rev. D* **2003**, *67*, 083509. [CrossRef]
18. Caldwell, R.R.; Kamionkowski, M.; Weinberg, N.N. Phantom energy: Dark energy with w < −1 causes a cosmic doomsday. *Phys. Rev. Lett.* **2003**, *91*, 071301.

19. Bouali, A.; Albarran, I.; Bouhmadi-López, M.; Ouali, T. Cosmological constraints of phantom dark energy models. *Phys. Dark Univ.* **2019**, *26*, 100391.
20. Bouali, A.; Albarran, I.; Bouhmadi-Lopez, M.; Errahmani, A.; Ouali, T. Cosmological constraints of interacting phantom dark energy models. *Phys. Dark Univ.* **2021**, *34*, 100907.
21. Dahmani, S.; Bouali, A.; Bojaddaini, I.E.; Errahmani, A.; Ouali, T. Smoothing the H_0 tension with a dynamical dark energy model. **2023**, arXiv:2301.04200.
22. Mhamdi, D.; Bargach, F.; Dahmani, S.; Bouali, A.; Ouali, T. Comparing phantom dark energy models with various diagnostic tools. *Gen. Rel. Grav.* **2023**, *55*, 11. [CrossRef]
23. Starobinsky, A.A. A new type of isotropic cosmological models without singularity. *Phys. Lett. B* **1980**, *91*, 99–102. [CrossRef]
24. Kerner, R. Cosmology without singularity and nonlinear gravitational Lagrangians. *Gen. Relativ. Gravit.* **1982**, *14*, 453–469. [CrossRef]
25. Nojiri, S.; Odintsov, S.D. Unified cosmic history in modified gravity: From F (R) theory to Lorentz non-invariant models. *Phys. Rep.* **2011**, *505*, 59–144. [CrossRef]
26. Nojiri, S.; Odintsov, S.; Oikonomou, V. Modified gravity theories on a nutshell: Inflation, bounce and late-time evolution. *Phys. Rep.* **2017**, *692*, 1–104. [CrossRef]
27. Bengochea, G.R.; Ferraro, R. Dark torsion as the cosmic speed-up. *Phys. Rev. D* **2009**, *79*, 124019. [CrossRef]
28. Linder, E.V. Einstein's Other Gravity and the Acceleration of the Universe. *Phys. Rev. D* **2010**, *81*, 127301. [CrossRef]
29. Bamba, K.; Geng, C.Q. Thermodynamics of cosmological horizons in f (T) gravity. *J. Cosmol. Astropart. Phys.* **2011**, *2011*, 008. [CrossRef]
30. Bamba, K.; Odintsov, S.D.; Sebastiani, L.; Zerbini, S. Finite-time future singularities in modified Gauss–Bonnet and (R, G) gravity and singularity avoidance. *Eur. Phys. J. C* **2010**, *67*, 295–310. [CrossRef]
31. de S. Silva, M.V.; Rodrigues, M.E. Regular black holes in f (G) gravity. *Eur. Phys. J. C* **2018**, *78*, 1–18.
32. Harko, T.; Lobo, F.S.; Nojiri, S.; Odintsov, S.D. f (R, T) gravity. *Phys. Rev. D* **2011**, *84*, 024020. [CrossRef]
33. Brans, C.; Dicke, R.H. Mach's principle and a relativistic theory of gravitation. *Phys. Rev.* **1961**, *124*, 925. [CrossRef]
34. Saez, D.; Ballester, V. A simple coupling with cosmological implications. *Phys. Lett. A* **1986**, *113*, 467–470. [CrossRef]
35. Duff, M.J. Kaluza-Klein theory in perspective. In *Proceedings of the Symposium: The Oskar Klein Centenary*; World Scientific: Singapore, 1994; pp. 22–35.
36. Hsu, S.D. Entropy bounds and dark energy. *Phys. Lett. B* **2004**, *594*, 13–16. [CrossRef]
37. Li, M. A model of holographic dark energy. *Phys. Lett. B* **2004**, *603*, 1–5. [CrossRef]
38. Hooft, G. Dimensional reduction in quantum gravity. *arXiv* **1993**, arXiv:gr-qc/9310026.
39. Susskind, L. The world as a hologram. *J. Math. Phys.* **1995**, *36*, 6377–6396. [CrossRef]
40. Wei, H.; Cai, R.G. A new model of agegraphic dark energy. *Phys. Lett. B* **2008**, *660*, 113–117. [CrossRef]
41. Gao, C.; Wu, F.; Chen, X.; Shen, Y.G. Holographic dark energy model from Ricci scalar curvature. *Phys. Rev. D* **2009**, *79*, 043511. [CrossRef]
42. Granda, L.; Oliveros, A. Infrared cut-off proposal for the holographic density. *Phys. Lett. B* **2008**, *669*, 275–277. [CrossRef]
43. Chen, S.; Jing, J. Dark energy model with higher derivative of Hubble parameter. *Phys. Lett. B* **2009**, *679*, 144–150. [CrossRef]
44. Granda, L.; Oliveros, A. New infrared cut-off for the holographic scalar fields models of dark energy. *Phys. Lett. B* **2009**, *671*, 199–202. [CrossRef]
45. Tsallis, C.; Cirto, L.J. Black hole thermodynamical entropy. *Eur. Phys. J. C* **2013**, *73*, 1–7. [CrossRef]
46. Tavayef, M.; Sheykhi, A.; Bamba, K.; Moradpour, H. Tsallis holographic dark energy. *Phys. Lett. B* **2018**, *781*, 195–200. [CrossRef]
47. Jahromi, A.S.; Moosavi, S.; Moradpour, H.; Graça, J.M.; Lobo, I.; Salako, I.; Jawad, A. Generalized entropy formalism and a new holographic dark energy model. *Phys. Lett. B* **2018**, *780*, 21–24. [CrossRef]
48. Saridakis, E.N.; Bamba, K.; Myrzakulov, R.; Anagnostopoulos, F.K. Holographic dark energy through Tsallis entropy. *J. Cosmol. Astropart. Phys.* **2018**, *2018*, 012. [CrossRef]
49. Ghaffari, S.; Moradpour, H.; Lobo, I.; Graça, J.M.; Bezerra, V.B. Tsallis holographic dark energy in the Brans–Dicke cosmology. *T Eur. Phys. J. C* **2018**, *78*, 1–9. [CrossRef]
50. Sheykhi, A. Modified Friedmann equations from Tsallis entropy. *Phys. Lett. B* **2018**, *785*, 118–126. [CrossRef]
51. Mohammadi, A.; Golanbari, T.; Bamba, K.; Lobo, I.P. Tsallis holographic dark energy for inflation. *Phys. Rev. D* **2021**, *103*, 083505. [CrossRef]
52. Cohen, A.G.; Kaplan, D.B.; Nelson, A.E. Effective field theory, black holes, and the cosmological constant . *Phys. Rev. Lett.* **1999**, *82*, 4971. [CrossRef]
53. Pavon, D.; Zimdahl, W. Holographic dark energy and cosmic coincidence. *Phys. Lett. B* **2005**, *628*, 206–210. [CrossRef]
54. Harrison, E. Hubble spheres and particle horizons. *Astrophys. J.* **1991**, *383*, 60–65. [CrossRef]
55. Sadjadi, H.M. The particle versus the future event horizon in an interacting holographic dark energy model. *J. Cosmol. Astropart. Phys.* **2007**, *2007*, 026. [CrossRef]
56. Wang, Y.; Xu, L. Current observational constraints to the holographic dark energy model with a new infrared cutoff via the Markov chain Monte Carlo method. *Phys. Rev. D* **2010**, *81*, 083523. [CrossRef]
57. Pradhan, A.; Kumar Singh, A.; Chouhan, D. Accelerating Bianchi type-V cosmology with perfect fluid and heat flow in Saez-Ballester theory. *Int. J. Theor. Phys.* **2013**, *52*, 266–278. [CrossRef]

58. Sharma, U.K.; Zia, R.; Pradhan, A. Transit cosmological models with perfect fluid and heat flow in Sáez-Ballester theory of gravitation. *J. Astrophys. Astron.* **2019**, *40*, 1–9. [CrossRef]
59. Sobhanbabu, Y.; Vijaya Santhi, M. Kantowski–Sachs Tsallis holographic dark energy model with sign-changeable interaction. *Eur. Phys. J. C* **2021**, *81*, 1–10. [CrossRef]
60. Collins, C. Tilting at cosmological singularities. *Commun. Math. Phys.* **1974**, *39*, 131–151. [CrossRef]
61. Coles, P.; Ellis, G. The case for an open universe. *Nature* **1994**, *370*, 609–615. [CrossRef]
62. Singh, C.; Zeyauddin, M.; Ram, S. Anisotropic Bianchi-V Cosmological Models in Saez-Ballester Theory of Gravitation. *Int. J. Mod. Phys. A* **2008**, *23*, 2719–2731. [CrossRef]
63. Naidu, R.; Aditya, Y.; Raju, K.D.; Vinutha, T.; Reddy, D. Kaluza-Klein FRW dark energy models in Saez-Ballester theory of gravitation. *New Astron.* **2021**, *85*, 101564. [CrossRef]
64. Mishra, R.; Dua, H. Bulk viscous string cosmological models in Saez-Ballester theory of gravity. *Astrophys. Space Sci.* **2019**, *364*, 195. [CrossRef]
65. Katore, S.; Shaikh, A. Hypersurface-homogeneous space-time with anisotropic dark energy in scalar tensor theory of gravitation. *Astrophys. Space Sci.* **2015**, *357*, 1–11. [CrossRef]
66. Santhi, M.V.; Sobhanbabu, Y. Bianchi type-III Tsallis holographic dark energy model in Saez–Ballester theory of gravitation. *Eur. Phys. J. C* **2020**, *80*, 1198. [CrossRef]
67. Berman, M.S.; de Mello Gomide, F. Cosmological models with constant deceleration parameter. *Gen. Relativ. Gravit.* **1988**, *20*, 191–198. [CrossRef]
68. Akarsu, Ö.; Dereli, T. Cosmological models with linearly varying deceleration parameter. *Int. J. Theor. Phys.* **2012**, *51*, 612–621. [CrossRef]
69. Bolotin, Y.L.; Cherkaskiy, V.; Lemets, O.; Yerokhin, D.; Zazunov, L. Cosmology in terms of the deceleration parameter. Part I. *arXiv* **2015**, arXiv:1502.00811.
70. Bouali, A.; Chaudhary, H.; Debnath, U.; Sardar, A.; Mustafa, G. Data Analysis of three parameter models of deceleration parameter in FRW Universe. *arXiv* **2023**, arXiv:2304.13137.
71. Bouali, A.; Chaudhary, H.; Mehrotra, A.; Pacif, S. Model-independent study for a quintessence model of dark energy: Analysis and Observational constraints. *arXiv* **2023**, arXiv:2304.02652.
72. Bouali, A.; Chaudhary, H.; Debnath, U.; Roy, T.; Mustafa, G. Constraints on the Parameterized Deceleration Parameter in FRW Universe. *arXiv* **2023**, arXiv:2301.12107.
73. Bouali, A.; Chaudhary, H.; Hama, R.; Harko, T.; Sabau, S.V.; Martín, M.S. Cosmological tests of the osculating Barthel–Kropina dark energy model. *Eur. Phys. J. C* **2023**, *83*, 121. [CrossRef]
74. Tiwari, R.K.; Beesham, A.; Shukla, B.K. Scenario of two-fluid dark energy models in Bianchi type-III Universe. *Int. J. Geom. Methods Mod. Phys.* **2018**, *15*, 1850189. [CrossRef]
75. Tiwari, R.; Beesham, A.; Shukla, B. Cosmological models with viscous fluid and variable deceleration parameter. *Eur. Phys. J. Plus* **2017**, *132*, 20. [CrossRef]
76. Tiwari, R.; Beesham, A.; Shukla, B. Behaviour of the cosmological model with variable deceleration parameter. *Eur. Phys. J. Plus* **2016**, *131*, 1–9. [CrossRef]
77. Tiwari, R.K.; Beesham, A.; Shukla, B.K. FLRW Cosmological Models with Dynamic Cosmological Term in Modified Gravity. *Universe* **2021**, *7*, 319. [CrossRef]
78. Handley, W.; Hobson, M.; Lasenby, A. PolyChord: Nested sampling for cosmology. *Mon. Not. R. Astron. Soc. Lett.* **2015**, *450*, L61–L65. [CrossRef]
79. Lewis, A. GetDist: A Python package for analysing Monte Carlo samples. *arXiv* **2019**, arXiv:1910.13970.
80. Foreman-Mackey, D.; Hogg, D.W.; Lang, D.; Goodman, J. emcee: The MCMC hammer. *Publ. Astron. Soc. Pac.* **2013**, *125*, 306. [CrossRef]
81. Gaztanaga, E.; Bonvin, C.; Hui, L. Measurement of the dipole in the cross-correlation function of galaxies. *J. Cosmol. Astropart. Phys.* **2017**, *2017*, 032. [CrossRef]
82. Kowalski, M.; Rubin, D.; Aldering, G.; Agostinho, R.; Amadon, A.; Amanullah, R.; Balland, C.; Barbary, K.; Blanc, G.; Challis, P.; et al. Improved cosmological constraints from new, old, and combined supernova data sets. *Astrophys. J.* **2008**, *686*, 749. [CrossRef]
83. Amanullah, R.; Lidman, C.; Rubin, D.; Aldering, G.; Astier, P.; Barbary, K.; Burns, M.; Conley, A.; Dawson, K.; Deustua, S.; et al. Spectra and Hubble Space Telescope light curves of six type Ia supernovae at 0.511 < z < 1.12 and the Union2 compilation. *Astrophys. J.* **2010**, *716*, 712.
84. Suzuki, N.; Rubin, D.; Lidman, C.; Aldering, G.; Amanullah, R.; Barbary, K.; Barrientos, L.; Botyanszki, J.; Brodwin, M.; Connolly, N.; et al. The Hubble Space Telescope cluster supernova survey. V. Improving the dark-energy constraints above z > 1 and building an early-type-hosted supernova sample. *Astrophys. J.* **2012**, *746*, 85. [CrossRef]
85. Betoule, M.; Kessler, R.; Guy, J.; Mosher, J.; Hardin, D.; Biswas, R.; Astier, P.; El-Hage, P.; Konig, M.; Kuhlmann, S.; et al. Improved cosmological constraints from a joint analysis of the SDSS-II and SNLS supernova samples. *Astron. Astrophys.* **2014**, *568*, A22. [CrossRef]

86. Scolnic, D.M.; Jones, D.; Rest, A.; Pan, Y.; Chornock, R.; Foley, R.; Huber, M.; Kessler, R.; Narayan, G.; Riess, A.; et al. The complete light-curve sample of spectroscopically confirmed SNe Ia from Pan-STARRS1 and cosmological constraints from the combined pantheon sample. *Astrophys. J.* **2018**, *859*, 101. [CrossRef]
87. Scolnic, D.; Brout, D.; Carr, A.; Riess, A.G.; Davis, T.M.; Dwomoh, A.; Jones, D.O.; Ali, N.; Charvu, P.; Chen, R.; et al. The Pantheon+ Type Ia Supernova sample: The full dataset and light-curve release. *arXiv* **2021**, arXiv:2112.03863.
88. Benisty, D.; Staicova, D. Testing late-time cosmic acceleration with uncorrelated baryon acoustic oscillation dataset. *Astron. Astrophys.* **2021**, *647*, A38. [CrossRef]
89. Hogg, N.B.; Martinelli, M.; Nesseris, S. Constraints on the distance duality relation with standard sirens. *J. Cosmol. Astropart. Phys.* **2020**, *2020*, 019. [CrossRef]
90. Martinelli, M.; Martins, C.J.A.P.; Nesseris, S.; Sapone, D.; Tutusaus, I.; Avgoustidis, A.; Camera, S.; Carbone, C.; Casas, S.; Ilić, S.; et al. Euclid: Forecast constraints on the cosmic distance duality relation with complementary external probes. *Astron. Astrophys.* **2020**, *644*, A80. [CrossRef]
91. Otalora, G.; Saridakis, E.N. Effective dark energy through spin-gravity coupling. *arXiv* **2022**, arXiv:2210.06598.
92. Sahni, V.; Saini, T.D.; Starobinsky, A.A.; Alam, U. Statefinder—A new geometrical diagnostic of dark energy. *J. Exp. Theor. Phys. Lett.* **2003**, *77*, 201–206. [CrossRef]
93. Capozziello, S.; Nojiri, S.; Odintsov, S.D. The role of energy conditions in f (R) cosmology . *Phys. Lett. B* **2018**, *781*, 99–106. [CrossRef]
94. Moraes, P.; Sahoo, P. The simplest non-minimal matter–geometry coupling in the f (R, T) cosmology. *Eur. Phys. J. C* **2017**, *77*, 1–8. [CrossRef]
95. Sahoo, P.K.; Sahoo, P.; Bishi, B.K. Anisotropic cosmological models in f (R, T) gravity with variable deceleration parameter. *Int. J. Geom. Methods Mod. Phys.* **2017**, *14*, 1750097. [CrossRef]
96. Sharif, M.; Fatima, H.I. Energy conditions for Bianchi type I universe in f (G) gravity. *Astrophys. Space Sci.* **2014**, *353*, 259–265. [CrossRef]
97. Capozziello, S.; Lobo, F.S.; Mimoso, J.P. Generalized energy conditions in extended theories of gravity. *Phys. Rev. D* **2015**, *91*, 124019. [CrossRef]
98. Santos, C.S.; Santos, J.; Capozziello, S.; Alcaniz, J.S. Strong energy condition and the repulsive character of f (R) gravity. *Gen. Relativ. Gravit.* **2017**, *49*, 1–14. [CrossRef]
99. Visser, M. General relativistic energy conditions: The Hubble expansion in the epoch of galaxy formation. *Phys. Rev. D* **1997**, *56*, 7578. [CrossRef]
100. Santos, J.; Alcaniz, J.; Rebouças, M. Energy conditions and supernovae observations. *Phys. Rev. D* **2006**, *74*, 067301. [CrossRef]
101. Bergliaffa, S.P. Constraining f (R) theories with the energy conditions. *Phys. Lett. B* **2006**, *642*, 311–314. [CrossRef]
102. Santos, J.; Alcaniz, J.; Reboucas, M.; Carvalho, F. Energy conditions in f (R) gravity. *Phys. Rev. D* **2007**, *76*, 083513. [CrossRef]
103. Santos, J.; Alcaniz, J.; Reboucas, M.; Pires, N. Lookback time bounds from energy conditions. *Phys. Rev. D* **2007**, *76*, 043519. [CrossRef]
104. SANTOS, J.; REBOUÇAS, M.J.; ALCANIZ, J.S. Energy conditions constraints on a class of f (R)-gravity. *Int. J. Mod. Phys. D* **2010**, *19*, 1315–1321. [CrossRef]
105. Gong, Y.; Wang, A. Energy conditions and current acceleration of the universe. *Phys. Lett. B* **2007**, *652*, 63–68. [CrossRef]
106. Schoen, R.; Yau, S.T. Proof of the positive mass theorem. II. *Commun. Math. Phys.* **1981**, *79*, 231–260. [CrossRef]
107. Hawking, S.W.; Ellis, G.F. *The Large Scale Structure of Space-Time*; Cambridge University Press: Cambridge, UK , 2023.
108. Caldwell, R.R. A phantom menace? Cosmological consequences of a dark energy component with super-negative equation of state. *Phys. Lett. B* **2002**, *545*, 23–29. [CrossRef]
109. Sahni, V.; Shafieloo, A.; Starobinsky, A.A. Two new diagnostics of dark energy. *Phys. Rev. D* **2008**, *78*, 103502. [CrossRef]
110. Sahoo, P.; Moraes, P.; Sahoo, P.; Ribeiro, G. Phantom fluid supporting traversable wormholes in alternative gravity with extra material terms. *Int. J. Mod. Phys. D* **2018**, *27*, 1950004. [CrossRef]